ELSEVIER

Isotopic characterisation and mobile detection of methane emissions in a heterogeneous UK landscape

Mounir Takriti [a,1,*], Susan E. Ward [a], Peter M. Wynn [a], Niall P. McNamara [b]

[a] *Lancaster Environment Centre, Lancaster University, Lancaster, LA1 4YQ, UK*
[b] *UK Centre for Ecology & Hydrology, Lancaster Environment Centre, Library Avenue, Lancaster, LA1 4AP, UK*

HIGHLIGHTS

- ^{13}C–CH_4 and ^2H–CH_4 measurements for natural and anthropogenic methane emissions.
- Emissions from landfills, natural gas, wetlands and agriculture were characterised.
- Improved separation of sources with ^2H measurements over ^{13}C only measurements.
- Mobile isotopic mapping identified individual sources in study area.
- Urban and agricultural land use show differences in isotopic patterns.

ARTICLE INFO

ABSTRACT

Characterising methane (CH_4) sources and their stable isotope values at the regional level is important for taking effective mitigation actions as well as more accurately constraining global atmospheric CH_4 budgets. We performed dual stable isotope (^{13}C, ^2H) analysis of CH_4 emission sources as well as mobile ^{13}C measurements in North-West England, in a region with a mix of natural and anthropogenic emission sources as well as potentially exploitable shale gas deposits. Dual isotope analysis was performed for enteric fermentation, animal waste, landfill gas, wetlands, and natural gas from the regional distribution network. Microbial emission sources' $\delta^{13}C$ values ranged from -72.1 ± 0.31‰ to -53.1 ± 1.17‰ with agricultural sources and landfills showing partially overlapping values (-65.3 ± 0.41‰ to -72.1 ± 0.31‰ and -59.2 ± 0.26‰ to -70.4‰, respectively). However, the use of a dual isotope approach with δ^2H provided additional separation between agricultural (-340 ± 0.8‰ to -322 ± 19.5‰) and landfill (-312 ± 0.3‰ to -282‰) CH_4. All microbial sources were clearly distinct from natural gas with mean values of -39.5 ± 1.38‰ and -184 ± 4.9‰ for $\delta^{13}C$ and δ^2H, respectively. Mobile measurements conducted over a distance of 557 km detected emissions from two out of four surveyed managed landfills in the region. Multiple gas leaks were detected, which may confound emissions from other thermogenic sources. When separating the surveyed area by land-use into agricultural and urban, we found that background levels of CH_4 were more depleted by around 1‰ in areas with agricultural land use compared to urban areas, but emissions from gas leaks and landfills are present in both categories. Our findings highlight the complexity of isoscapes in regions with multiple types of emission sources and the value of dual-isotope measurements in source attribution.

1. Introduction

Atmospheric concentrations of methane (CH_4) have increased by a factor of 2.6 since pre-industrial times, and it contributes around 23% (0.62 W m^{-1}) to the additional radiative forcing in the lower atmosphere

(Etminan et al., 2016; Saunois et al., 2020). Rapidly reducing CH_4 emissions is now internationally recognised as key to achieving the goal of limiting global warming to 1.5 °C (www.globalmethanepledge.org). Increasing atmospheric concentrations of CH_4 are mainly attributed to increased emissions from agriculture, natural gas production, and

---

wetlands, although the relative contribution from these sources is still debated (e.g. Allen, 2016; Hmiel et al., 2020; Saunois et al., 2016; Turner et al., 2017). It is established, however, that over 50% of total CH_4 emissions are anthropogenic (Saunois et al., 2020), and due to the short lifetime of atmospheric CH_4 there is significant potential to reduce radiative forcing over decadal timescales by cutting emissions (Shindell et al., 2012).

The main anthropogenic sources of CH_4 emissions are enteric fermentation from ruminants, storage and spreading on fields of animal waste, rice cultivation, waste management, and fugitive emissions from natural gas infrastructure. The latter can occur during the extraction and processing stages as well as distribution through the pipeline network from storage facilities to end users. Fugitive natural gas emissions are estimated to account for around 1% of total natural gas production, though estimates across the supply chain vary widely (Balcombe et al., 2017). Mobile measurements have shown that gas leaks from mains pipelines are common in at least some US cities, occasionally reaching hazardous levels (Fischer et al., 2017; Jackson et al., 2014; Phillips et al., 2013; Weller et al., 2018), while direct measurements from other regions are still more limited (e.g. Lowry et al., 2020; Zazzeri et al., 2017; Xueref-Remy et al., 2019). The rapid expansion of natural gas production through hydraulic fracturing in the USA has raised concerns over its environmental impacts, including fugitive emissions, and spurred the development of mobile measurement approaches for emission detection and quantification (Albertson et al., 2016; Brantley et al., 2014; Rella et al., 2015).

Despite increasing availability of atmospheric measurements, sourced from ground based, airborne and remote sensing techniques, efforts to attribute and limit anthropogenic emissions are still hampered by uncertainty around spatially and temporally heterogeneous emissions at local and regional scales. Total emissions at a given scale are either estimated by top-down or bottom-up approaches. In top-down approaches, data from atmospheric measurements are used to model emission rates. However, the co-occurrence of multiple emission sources in the landscape makes it challenging to disentangle their relative contributions. In contrast, bottom-up estimates are based on upscaling emission measurements from individual locations of known emission source categories. These are dependent on detailed awareness of emission sources in the focus area, and the accuracy of emission factors. Moreover, bottom up emission estimates are often not in agreement with top-down atmospheric measurements (Allen, 2014; Kirschke et al., 2013).

The main tool for attributing emissions to sources is stable isotope analysis, as emission categories have different isotopic signatures (e.g. Allen, 2016; Feinberg et al., 2018; Kirschke et al., 2013; Schwietzke et al., 2016). For example, microbial emissions from anaerobic respiration in ruminants, wetlands, and organic waste, are isotopically lighter in their stable carbon (C) isotope ratios ($^{13}C/^{12}C$) compared to natural gas from thermogenic sources (Whiticar, 1999). However, it has been shown that there are considerable geographic variations in the isotopic signatures of CH_4 emissions, due to factors such as differences in fossil fuel formation (Liu et al., 2019), latitudinal trends in wetland emissions signatures (Ganesan et al., 2018), use of C_3 vs C_4 plants in livestock fodder (Chang et al., 2019), or climate differences and management practices in waste management (Chanton et al., 2008). Use of stable isotopes to constrain CH_4 emissions therefore requires an accurate knowledge of regional emission signatures, both for regional and global estimates (Feinberg et al., 2018).

Isotopic characterisation of CH_4 sources is quite uneven. The database of Sherwood et al. (2017) contains 120 references for fossil sources, but only 41 for all non-fossil sources combined. In addition, the majority of research to date has focussed on the C isotopes of CH_4, with only 11 references for non-fossil sources reporting H isotope values. Hydrogen isotopes can help distinguish between certain emission sources that overlap in their carbon isotope signatures, for example the two main pathways of microbial CH_4 formation, acetoclastic and hydrogenotrophic methanogenesis (Whiticar, 1999). Measurements of H-isotope source signatures can provide further constraints on atmospheric CH_4 budgets and more observations are needed as parameters for model studies (Ganesan et al., 2019).

Mobile measurements, enabled by recent advances in spectroscopic analyser technology, are a relatively new approach to identifying CH_4 emission sources at the regional level, and combine high spatial resolution with a comparatively large coverage. Mobile measurements have been successfully used for identifying emissions from different sources, including beef and dairy farming, oil and gas production, landfills, and pipeline leaks (Fischer et al., 2017; Lopez et al., 2017; Lowry et al., 2020; Phillips et al., 2013; Weller et al., 2018; Xueref-Remy et al., 2020; Zazzeri et al., 2015). Linking mobile measurements of CH_4 concentration with isotopic analysis can help attribute emissions to sources which would otherwise have an ambiguous origin.

Our research focusses on the Fylde peninsula and Morecambe Bay area in North West England, an area that on a small scale combines intensive agricultural use with urban environments and coastal wetlands, natural gas infrastructure, and both managed and historic landfill sites. The area therefore has a range of different natural and anthropogenic methane sources, and it is also among the first regions outside the USA where hydraulic fracturing to extract shale gas has been explored. This area poses particular challenges to attributing (fugitive) CH_4 emissions. The approved drill sites for shale gas extraction are mostly surrounded by dairy and cattle farmland and there are natural gas pipeline distribution networks and multiple landfills throughout the area. This means that there is potential for confounding pre-existing emission sources with emissions related to gas extraction, particularly when only relying on concentration measurements without the use of tracers such as CH_4 stable isotopes or other hydrocarbons co-emitted with CH_4.

Our aims for this study were to regionally 1) determine the dual-isotopic signatures ($\delta^{13}C$ and $\delta^{2}H$) of the major CH_4 source categories 2) identify and attribute CH_4 emission sources in the region 3) identify emission and stable isotope patterns related to land use. To this end, we performed three studies: 1) We collected gas samples at source from a range of regional emission sources and measured their dual-isotope values using high precision IRMS analysis; 2) we performed mobile surveys to identify and map regional emission sources and used mobile $\delta^{13}C$ measurements to attribute larger emissions to source categories; 3) we combined mobile measurement data with land use classification maps to investigate spatial patterns.

2. Methods

2.1. Study area

The study was conducted in England on the Fylde peninsula (53°50′ N, 2°54′ W), south of the city of Lancaster (54°3′N, 2°48′W) and the area surrounding Morecambe Bay (54°7′N, 2°53′W), along the coast of the Irish Sea (see Fig. 2). Land use in the Fylde area is dominated by dairy and cattle farming and the urban areas of Blackpool and Fleetwood along the coast. At the time of sampling, there were four actively managed municipal landfills in the study area, which have gas extraction systems to capture produced CH_4. There are numerous, mostly small, historic landfills, though information is limited for sites that existed before landfills were regulated (Environment Agency, 2018). The Morecambe Bay area (Fig. 3) north of Lancaster is again dominated by livestock farming with marshlands along parts of the coast as well as a peatland. On the north-western side of the Morecambe Bay is the Barrow Gas Terminal (54° 5′47″N, 3°10′50″W) which processes gas from the Morecambe Bay gas fields off the coast (Fig. 4).

2.2. Stable isotope notation

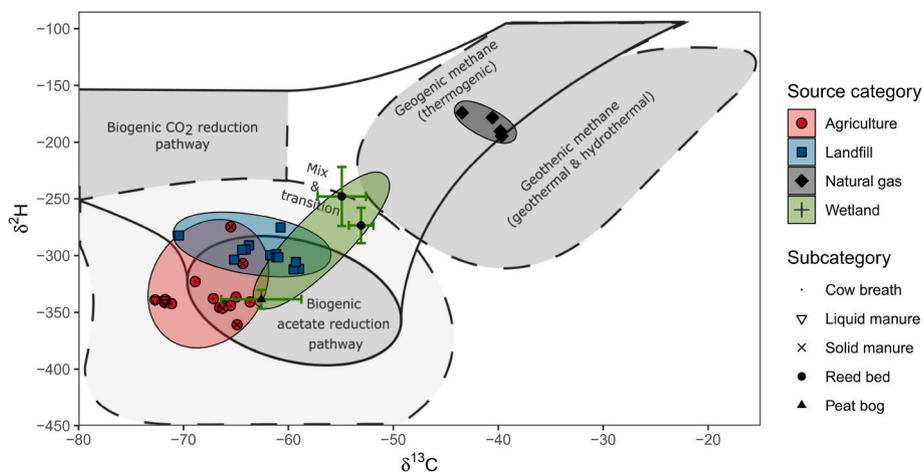All stable isotope values reported in this study are presented using

Fig. 1. Genetic characterisation plot of δ^2H-CH$_4$ versus δ^{13}C-CH$_4$ values in this study relative to genetic domains, indicated by shaded areas, developed by Whiticar (1999). Wetland data is based on Miller-Tans plots with error bars representing the standard error of the regression slope.
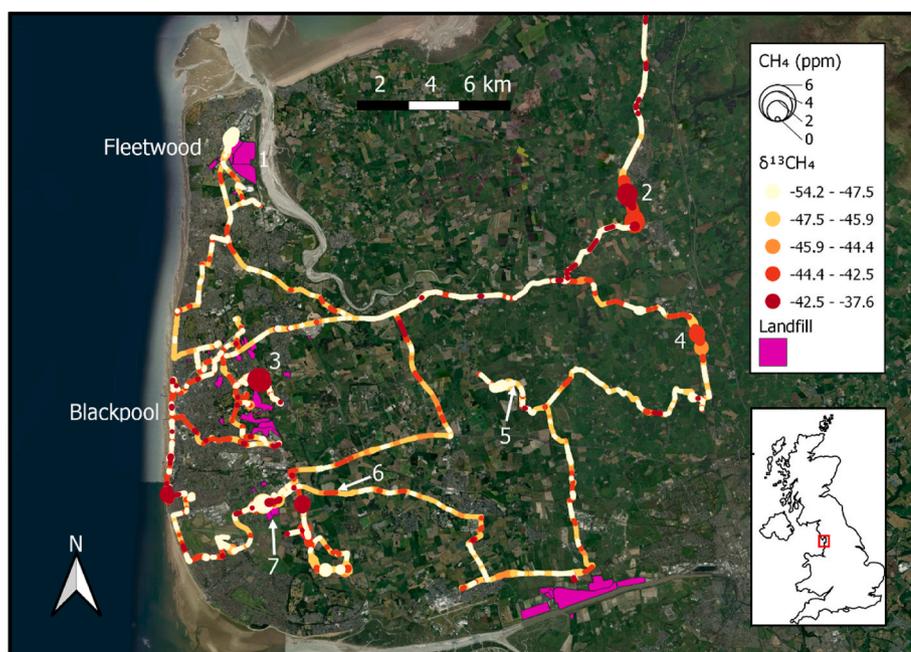

Fig. 2. Map of mobile measurements in the Fylde area. Map insert highlights the study area within the UK. Symbol width indicates CH$_4$ concentration above background as measured by a UGGA. Colour indicates 30 s running mean δ^{13}C values measured by a G2201-*i* isotopic gas analyser and grouped by variance into 5 ranges. Numbered locations refer to CH$_4$ emission plumes listed in Table 1 and drilling sites: 1 Jameson Rd landfill, 2 Preston Lancaster New Rd, 3 Newton Dr, 4 Garstang Rd, 5 Roseacre Wood drilling site, 6 Preston New Rd drilling site, 7 Midgeland Farm landfill. Satellite image source: Earthstar Geographics.

the δ-notation, i.e. the relative difference, in per mille (‰), of heavy and light isotopes between a sample and a standard: $\delta = [(R_{Sample}/R_{Standard}) - 1] \times 1000$, where R is the ratio of heavy and light isotopes, i.e. ^{13}C/^{12}C or ^{2}H/^{1}H. Values are reported relative to the international standards Vienna Peedee Belemnite (VPDB) for C and Vienna Standard Mean Ocean Water (VSMOW) for H. Errors are reported as standard errors of the mean, unless stated otherwise.

2.3. Characterisation of emission sources

2.3.1. Wetlands

Samples were collected at two wetland sites in the Morecambe Bay area: At Leighton Moss RSPB reserve, a coastal reed bed (54°10′7″N, 2°47′39″W), and at Roudsea Wood and Mosses National Nature Reserve, a lowland raised peat bog (54°14′5.70″N, 3°1′24.04″W). At Leighton Moss, samples were collected within the reed bed in June and September 2015 from sites with different vegetation structure: grass dominated, moss dominated, and mostly bare ground in the process of being colonised by young reeds. Due to conservation management practices at

the site, two equivalent locations with similar vegetation structure were selected for the two samplings. At Roudsea Wood, samples were collected in August 2015. Two dominant vegetation types, heather and moss, were selected.

For each vegetation type, three replicate samples were collected via gas flux chambers. A 30 cm diameter 10 cm high gas sampling chamber collar was installed for each replicate to a depth of around 5 cm. Collars were sealed with opaque 19 L dome-shaped chambers and the CH$_4$ concentration in each chamber was measured for a minimum of 5 min using a Los Gatos Research Ultraportable Greenhouse Gas Analyzer measuring CO$_2$, CH$_4$, and H$_2$O (henceforth UGGA, Los Gatos Research Inc., San Jose, USA). Flux rates were calculated from the rate of CH$_4$ concentration change as described in McEwing et al. (2015) and based on a minimum of 30 s of continuous measurements. To ensure consistent treatment of data and exclusion of anomalous ebullition events, data was treated following the DEFRA SP1210 protocol (Evans et al., 2017).

At the end of the UGGA flux measurements, chambers were left on the collars for a total of 15–40 min, depending on flux rates (see Table S2), to allow gas concentrations to build up to the necessary
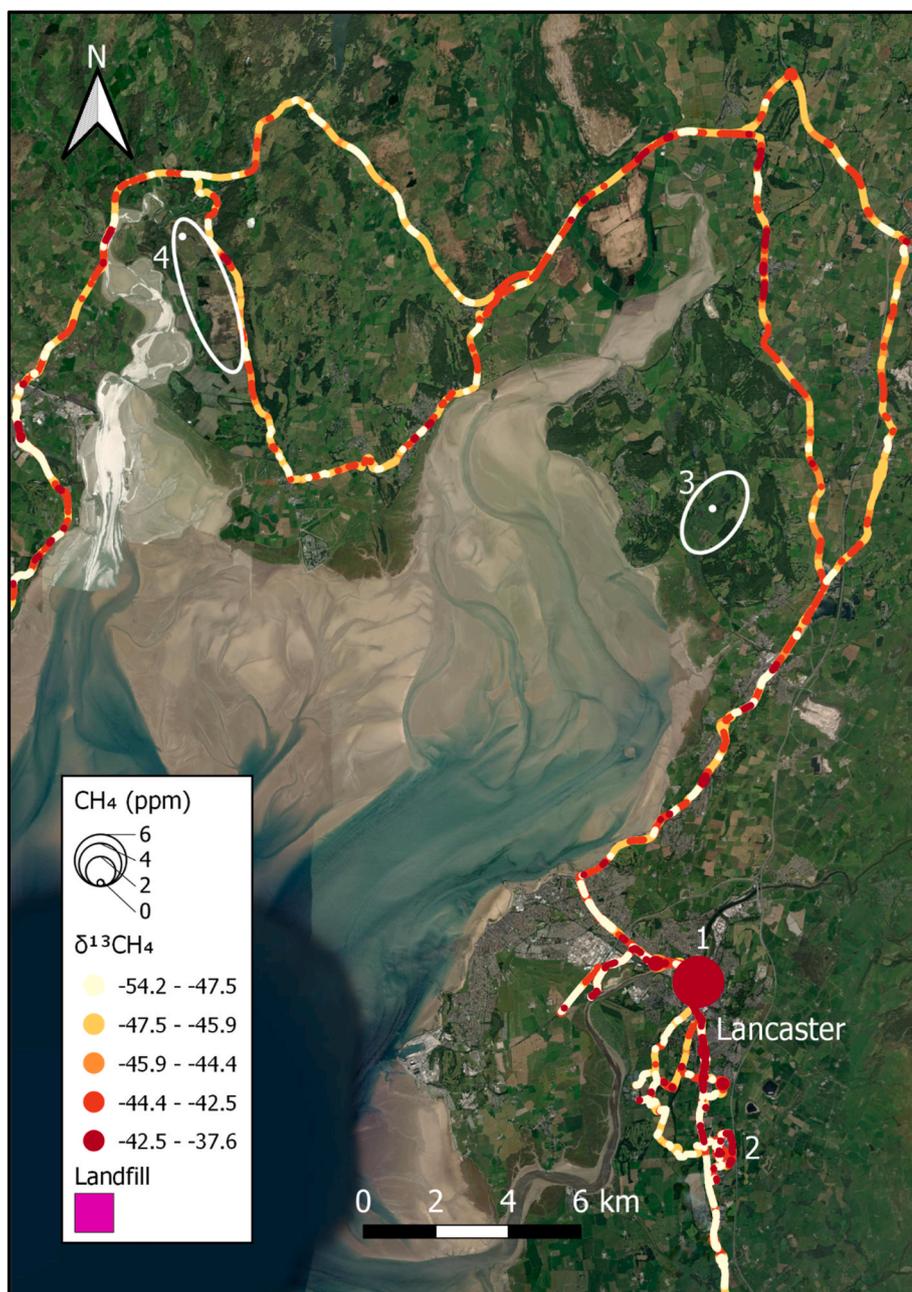
Fig. 3. Map of mobile measurements around Lancaster and Morecambe Bay. Symbol width indicates CH_4 concentration above background as measured by a UGGA. Colour indicates 30 s running mean $\delta^{13}C$ values measured by a G2201-*i* isotopic gas analyser and grouped by variance into 5 ranges. Numbered locations: 1 Cable St, Lancaster (see Table 1), 2 Lancaster University, 3 Leighton Moss RSPB Nature Reserve, 4 Roudsea Wood Nature Reserve. Points in locations 3 and 4 mark sampling sites. Satellite image source: Earthstar Geographics.

concentration for isotopic analysis. Headspace samples were then extracted with a syringe through the chamber septa and transferred to evacuated Exetainer vials (Labco Limited, Lampeter, UK) for concentration and isotopic analysis.

2.3.2. Landfill sites

Samples were collected at two managed landfill sites in the Fylde area, Clifton Marsh Landfill Site (53°45′2″N, 2°48′49″W) and Jameson Road Landfill Site (53°54′14″N, 3°0′59″W). In both sites, the non-operational parts are capped and both sites have gas extraction systems and use landfill gas for energy generation. Gas samples were collected in 1 L Tedlar gas sampling bags (Adtech Polymer Engineering Ltd., Gloucestershire, UK) which were flushed with hydrocarbon free air and evacuated before use. For sample collection, the Tedlar bags were connected to valves in the manifolds of the gas collection system and passively filled with landfill-gas.

Samples for isotopic analysis were transferred on the same day to

evacuated Exetainer vials via syringe. Chamber flux measurements on capped sections of the landfills were performed as described above, for a total of nine replicates at each site. No significant fluxes were detected during those measurements, data were therefore excluded from further analysis.

2.3.3. Agricultural sources

Samples of emissions from cow-breath, liquid manure, and solid manure were collected at Myerscough College's Lodge Farm (53°51′4″N, 2°46′36″W) in March and August 2015. Samples from eight beef and dairy cows on a C_3 diet were collected. To collect the breath samples, we used a vacuum sampling device to fill air into a Tedlar gas sampling bag: The Tedlar bag was placed into an airtight box and the box was connected to a hand pump and evacuated to draw air into the bag. The valve of the bag was connected, through the box's lid, to a tube with a funnel attached to it. Air was pumped into the bag while holding the funnel in front of the cows' mouths. Emissions from liquid manure

Fig. 4. Map of mobile measurements around Barrow-in-Furness. Symbol width indicates CH_4 concentration above background as measured by a UGGA. Colour indicates 30 s running mean $\delta^{13}C$ values measured by a G2201-*i* isotopic gas analyser and grouped by variance into 5 ranges. Numbered locations: 1 Roose Rd, 2 Rampside Gas Terminal with emissions measured to the East at Rampside Rd, see Table 1. Satellite image source: Earthstar Geographics.

were sampled by using the vacuum sampling device to take air samples above a ventilation hole in a collection pit. Samples for stable isotope and concentration analysis were transferred from Tedlar sampling bags to evacuated Exetainers on the same day. The solid manure emissions were sampled by placing a gas flux chamber on the solid manure and, after letting the gas build up for several minutes, collecting a sample through the chamber septum with a syringe.

2.3.4. Natural gas

To obtain isotope values of natural gas that were representative for the local gas distribution network, we sampled gas from a laboratory gas outlet at Lancaster University. Samples were collected at multiple timepoints between 2015 and 2017 to capture changes in gas composition over time, and specifically at times of mobile sampling campaigns. For each sampling, a Tedlar bag was attached to the outlet and filled with gas. Gas samples were transferred to Exetainer vials for subsequent isotopic analysis.

2.3.5. Gas analysis

For CH_4 concentration analysis, 10 mL gas samples were transferred via syringe into evacuated 3 mL Exetainer vials. Gas concentrations were measured by gas chromatography using an Autosystem XL GC (Perkin-nElmer, Waltham, MA, USA) as described in Case et al. (2014). Stable isotope analysis of CH_4 was performed at UC Davis Stable Isotope Facility (SIF) (University of California, Davis, USA). For all $\delta^{13}CH_4$ analysis, and analysis of δ^2H of samples ≥ 4 ppm, 20 mL gas samples were transferred to 12 mL Exetainer vials. For δ^2H analysis of samples with <4 ppm CH_4, 100 mL samples were transferred into 100 mL Wheaton serum bottles with crimp caps to achieve sufficient sample volume for analysis. Analysis was performed by gas chromatography-combustion/pyrolysis-isotope-ratio mass spectrometry as described in Yarnes (2013) with a precision (1 SD) of 0.2‰ for $\delta^{13}C$ and 2‰ for δ^2H.

2.4. Mobile measurements

Potential CH_4 emission sources in the study area were selected for mobile measurements, including landfills, farms, wastewater treatment

plants, and the Barrow Gas Terminal. In addition, two proposed drill sites for shale gas exploration, Preston New Road and Roseacre Wood (Fig. 2), as well as randomly selected urban and coastal locations not nearby any known emission sources were chosen. Where road access permitted, we selected multiple points around each potential emission source to maximise the chance of downwind measurements under different wind conditions. A route connecting all points for each campaign was selected using a genetic algorithm to optimise driving distance.

A full description of the mobile measurement system and its validation is provided in Takriti et al. (2021). In brief, a vehicle was equipped with two gas analysers, a Picarro G2201-*i* isotopic gas analyser (Picarro Inc. Santa Clara, USA) for $\delta^{13}C$ measurements (henceforth G2201-*i*), and the UGGA. Both instruments measure CO_2, CH_4, and H_2O concentration in air, while the UGGA's faster response time gives more accurate values for rapidly changing ambient concentrations with a difference of around 40% in measured peak amplitudes (Takriti et al., 2021). The air inlet was mounted on the roof of the vehicle. The output of each analyser and the anemometer (see below) was broadcast via Wi-Fi to two tablet devices mounted in front of the passenger seat to monitor measurements in real time. The system was powered by a total of six deep cycle batteries providing enough charge to operate the system for over 10 h of continuous measurements. Location and speed were measured by a R330 GNSS Receiver with a Hemisphere A21 Antenna (Hemisphere GNSS Inc., Arizona, USA) mounted on the vehicle roof providing location data with a nominal accuracy of ≤ 0.5 m. Wind speed and direction were measured using a roof mounted WindMaster PRO 3-Axis Ultrasonic Anemometer (Gill Instruments Ltd., Hampshire, UK), and data from both instruments was recorded to a datalogger (Campbell, UK). Vehicle speed and direction were calculated based on GPS data. Wind speed and direction were calculated for each measurement point by correcting the wind vector for the orientation of the vehicle and subtracting the vehicle movement from the wind vector (see Supplementary Information in Takriti et al. (2021) for calculations).

Before surveys, the gas analysers were calibrated for concentration using certified BOC gas standards (BOC Ltd., Guildford, UK) introduced through the system's air inlet. The G2201-*i* was calibrated for $\delta^{13}C$

before surveys using isotopic CH$_4$ standards with −23.9‰, −54.5‰, and −66.5‰ diluted to around 5 ppm (Isometric Instruments, Victoria, Canada), covering the range of expected isotope ratios in the study area. Calibration standards were measured for 10 min each. To correct for instrument drift, a reference gas cylinder was mounted in the vehicle and gas was run through the sampling system at the start, once during, and after each day of the sampling campaign for 10 min each. For individual sampling days, the standard deviations for mean reference CH$_4$ concentration measurements were 4 ppb for the UGGA and 0.9 ppb for the G2201-*i*, on average. Mean precision of δ^{13}C measurements for individual sampling days was 0.74‰. Across all sampling days, concentration and isotopic precision were 14 ppb, 13 ppb, and 0.74‰, respectively.

Measurements were taken during the daytime on a total of four days in November 2016, and February and March 2017. When elevated CH$_4$ emissions where detected, the vehicle was stopped for around 10 min, traffic conditions permitting, to take more precise isotopic measurements. Measurements were collected over a total of 557 km at a mean speed of 42 km h^{-1}.

2.5. Data analysis

2.5.1. Isotope source characterisation

Wetland isotopic source values were estimated using Miller-Tans plots (Miller and Tans, 2003) with standard major axis regression models. One datapoint from the June measurements at Leighton Moss was removed where CH$_4$ concentration in the chamber was over 650 ppm and over four times the next highest value. For samples of animal waste emissions, dilution with background air was corrected using a simple linear mixing model.

2.5.2. Mobile data analysis

To estimate variability in mobile background measurements under real-world conditions, we selected observations from locations away from known or observed emission sources (n = 10,029). The average standard deviation across all these observations was 0.0027 ppm (2.7 ppb) for the G2201-*i* and 0.0033 ppm (3.3 ppb) for the UGGA.

While the instruments are therefore able to detect relatively minor changes in atmospheric CH$_4$ concentration, such small variations are difficult to interpret in practice. For the purpose of this study we have therefore limited analysis of elevated CH$_4$ concentrations to peaks with a minimum amplitude of 10% above a moving background as defined in Takriti et al. (2021).

To simultaneously visualise both the more accurate UGGA CH$_4$ concentration data and the G2201-*i* δ^{13}C data, an offset of 8 s was applied to the UGGA data to, on average, align the maximum amplitude of the peaks of each instrument (Figs. 2–4). All other analyses were performed independently on the unadjusted data.

Mobile concentration measurements can underestimate true atmospheric concentrations due to lag in instrument response and can vary depending on instrumental setup. We therefore also calculated the speed corrected peak area i.e. the integral of concentration above background and distance travelled as a setup-independent parameter (Takriti et al., 2021).

The isotope signature of peaks was determined from Miller-Tans plots as the slope of a regression of the product of CH$_4$ concentration and δ^{13}C-value against CH$_4$ concentration. For the regression we used York's method to obtain unbiased estimates of the regression parameters that allow for errors in both variables and produce an uncertainty estimate that is based on the empirical instrument precision (Wehr and Saleska, 2017; York, 1969). Most of the detected peaks were too small to confidently determine the isotopic signature. As a threshold, we used a standard error (SE) of the slope of 6‰, values above that were not considered for isotopic analysis. This level of precision allowed for distinguishing between CH$_4$ from microbial and thermogenic sources whose mean δ^{13}C signatures differ by around 15–25‰ on average

(Fig. 1). For major peaks, we aimed to identify the emission source based on location, isotope signature, and wind direction at the time of measurement.

2.6. Spatial analysis of emissions and land use

To investigate links between emissions and land use, we used the British Land Cover Map 2015 (Rowland et al., 2017) to assign each mobile observation to a land use type. Observations assigned to either urban or agricultural land use, two dominant forms of land use in the study area with contrasting emission sources, were included in the analysis. For this study, land classified as "improved grassland" (mainly used for grazing with potential manure application) and "arable and horticulture" (potential manure application) were grouped as agricultural land. Built up areas are classified as either "urban" or "suburban". Since suburban land is often intermixed with other land cover and tends to form a buffer between more densely populated urban land and agricultural land, it was excluded from the analysis (Figure S4). Together urban and agricultural land covers make up 69% of the study area (Table S3). Emission δ^{13}C signatures for the study area were determined using Miller-Tans plots excluding stationary data to avoid bias towards longer measurements for some sources.

This is a simplified categorisation as the agricultural land use group is heterogeneous, built-up areas are dispersed within agricultural land and mixing will occur between the two. However, our main aim was to distinguish broadly between more densely populated urban areas (4.0% of land cover in the study area) where we expected upwind emissions to be more strongly dominated by leaks from natural gas pipelines and traffic emissions, and agricultural land (65% of land cover in the study area) where we expected upwind emissions to be more strongly dominated by enteric fermentation from cows and sheep as well as manure storage and application. While the urban area as a percentage of the total study area was small, a disproportionate amount of sampling was performed in urban areas (Fig. S4, Table S4).

2.7. Software

All data processing and analysis were performed in R version 4.0.5 (R Core Team, 2021), with the additional use of the IsoplotR (Vermeesch, 2018), fossil (Vavrek, 2011), lmodel2 (Legendre, 2018), and geosphere (Hijmans, 2017) packages. Mapping of mobile measurements and spatial analysis were performed using QGIS Geographic Information System version 3.20.1 (QGIS Development Team, 2021).

3. Results

3.1. Fylde isotopic source characterisation

Our sampled source categories in the Fylde area showed a clear distinction between microbial sources and natural gas (Fig. 1, Table S1). The δ^{13}C value for individual natural gas samples ranged from −43.5‰ to −33.1‰ while values for microbial sources ranged from −72.1‰ to −53.1‰. Similarly, natural gas was more enriched in ^{2}H with δ-values between −195‰ and −174‰, while mean microbial sources ranged from −361‰ from solid manure to −248‰. For both ^{13}C and ^{2}H, the most depleted values were found in animal waste, while the most enriched values were found in the emissions from the coastal reed bed at Leighton Moss (Fig. 1). The mean values for the sampled landfills, agricultural sources, and Roudsea Wood (the lowland raised peat bog), overlapped in their δ^{13}C signatures, with agricultural sources being more depleted, on average (Table S 1). A clearer distinction between agricultural sources and landfills was found in the mean δ^{2}H values, as landfills were more depleted in δ^{2}H by around 35‰. Between the two wetland sites, Roudsea Wood showed δ^{2}H values over 60‰ more depleted than Leighton Moss, depending on sampling date.

3.2. Mobile CH$_4$ source identification and land use

We surveyed a total of 557 km of road, of which 72 km fall within urban and 238 km fall within agricultural areas (Table S3). Background concentrations throughout the study area averaged 1.97 ppm CH$_4$ (Table S4). Background δ^{13}C values were −45.0 ± 3.7‰ (mean ± SD) for urban and −46.0 ± 3.8‰ for agricultural areas. Observed wind speeds during surveys ranged from 0.01 to 21.7 m s^{-1}, with a mean of 3.6 m s^{-1} and a median of 2.8 m s^{-1}.

We measured a total of 32 peaks >10% above background, as measured with the G2201-*i*, and a total of 55 peaks with the UGGA. Maximum concentrations measured were 5.6 ppm for the G2201-*i* and 8.0 ppm for the UGGA. This discrepancy is due to the difference in measurement speed between the two instruments. The median of the peak area, i.e. the integrated CH$_4$ concentration over the distance driven, as measured by the G2201-*i*, was 150.18 ppm m and 543.82 ppm m for urban and agricultural areas, respectively. Peak area was heavily right skewed with many small and a few large peaks (Fig. S1).

We detected notable emissions at eight locations where the isotopic signature could be determined within ±6‰. In each case, isotope and wind data indicate an anthropogenic source (Table 1, Figs. 2–4). We found emissions from two of the four landfill sites with gas extraction systems that were surveyed. Five plumes with δ^{13}C < 40‰ are likely attributable to gas pipeline leaks, an average of one leak per 112 km driven. One plume with a heavily enriched, thermogenic ^{13}C signature was detected next to the Barrow Gas Terminal. While elevated concentrations of up to 0.56 ppm above background were observed near cow barns and near fields with recent slurry spreading, isotopic signatures for these emissions could not be determined with sufficient accuracy.

The two landfill sites were the only emission sources in the study area whose isotopic signature could be identified as microbial with a combined δ^{13}C source signature of −59.4‰. The remaining elevated concentrations are dominated by isotopically enriched emissions with an overall δ^{13}C source signature of −33.9‰ (Fig. 5).
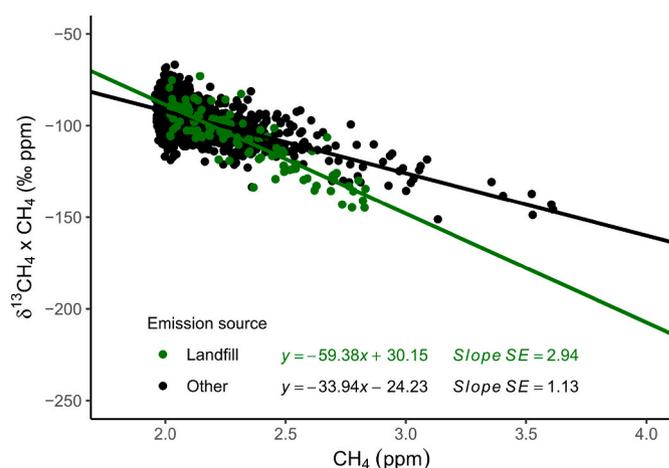

Fig. 5. Miller-Tans plot for elevated CH$_4$ data across land use types, excluding stationary measurements (n = 1170). A separate regression was calculated for known emissions from landfill sites (n = 118).

4. Discussion

4.1. Isotopic source characterisation

The emission signatures found in this study are within the broad range of values reported for thermogenic and microbial sources (Fig. 1, Whiticar, 1999).

The two wetland sites showed distinct isotope values. At Leighton Moss, the coastal reed bed, δ^{13}C and δ^{2}H values were enriched relative to the values at Roudsea Wood, the lowland raised peat bog, by up to 9‰ and 90‰, respectively. Stable isotope values of wetland CH$_4$ emissions depend on wetland ecology and follow broad latitudinal trends (Ganesan et al., 2018). In this case, both sites are situated near the coast and less than 17 km apart, experiencing almost identical climatic conditions. Differing CH$_4$ isotope values must therefore be the result of specific environmental conditions, such as vegetation, redox chemistry, and trophic status. For example, δ^{13}C emissions from minerotrophic

Table 1

Major CH$_4$ plumes identified in the study area with δ^{13}C signature SE < 6.0‰ determined using a G2201-*i* isotopic gas analyser.

Location	Date	Source	Coordinates	Max CH$_4$ (ppm)	Peak height (ppm)	δ^{13}CH$_4$ ± SE (‰)	Peak area (ppm s)	Peak area (ppm m)[a]
Midgeland Farm landfill, Blackpool	Feb 2017	Landfill	53° 46′ 54″ N, 3° 0′ 0″ W	2.82	0.83	−59.7 ± 4.83	59	834
Midgeland Farm landfill, Blackpool[b]	Feb 2017	Landfill	53° 46′ 54″ N, 2° 59′ 60″ W	2.74	0.74	−62.4 ± 5.68	25	416
Jameson Rd Landfill, Fleetwood	Feb 2017	Landfill	53° 54′ 40″ N, 3° 1′ 21″ W	2.83	0.83	−59.5 ± 4.75	47	640
Staining Rd, Blackpool	Feb 2017	Gas leak	53° 49′ 32″ N, 3° 0′ 14″ W	3.84	1.84	−35.3 ± 1.01	1007	n.a.
Cable St, Lancaster	Nov 2016	Gas leak	54° 3′ 5″ N, 2° 47′ 51″ W	5.59	3.63	−34.2 ± 0.69	1073	n.a.
Cable St, Lancaster[b]	Nov 2016	Gas leak	54° 3′ 5″ N, 2° 47′ 51″ W	4.59	2.64	−34.7 ± 1.30	608	n.a.
Preston Lancaster New Rd, Garstang[c]	Feb 2017	Gas leak	53° 53′ 34″ N, 2° 47′ 6″ W	3.03	1.06	−33.5 ± 2.72	79	1348
Preston Lancaster New Rd, Garstang[b,c]	Feb 2017	Gas leak	53° 52′ 59″ N, 2° 46′ 50″ W	2.57	0.58	−30.8 ± 5.74	38	662
Myerscough Planks, Barton	Feb 2017	Gas leak	53° 50′ 38″ N, 2° 44′ 33″ W	2.53	0.57	−28.1 ± 5.27	42	657
Roose Rd, Barrow-in-Furness	Mar 2017	Gas leak	54° 6′ 40″ N, 3° 12′ 22″ W	2.38	0.44	−29.5 ± 5.89	84	n.a.
Rampside Rd, Barrow-in-Furness	Mar 2017	Gas terminal	54° 6′ 20″ N, 3° 10′ 32″ W	2.92	0.97	−23.7 ± 1.93	373	n.a.

[a] Peak areas corrected for driving speed calculated as the product of peak are in ppm s and speed in m s^{-1}, see Takriti et al. (2021); n.a. denotes stationary measurements.

[b] Second measurement from the same location as previous row.

[c] Location and isotope data indicate overlapping plumes from two gas leak.

wetlands have been shown to be more enriched than those of ombrotrophic wetlands (Hornibrook and Bowes, 2007).

Our local natural gas $\delta^{13}C$ values of $-39.5 \pm 1.38‰$ are considerably more enriched than the national mean for oil and gas of $-47.4 \pm 1.76‰$ as reported by Sherwood et al. (2017), but in good agreement with the mean value of $-41‰$ reported by Lowry et al. (2020) for the area. While our data only include samples of network gas, these are likely the major contributor to fugitive natural gas emissions in the study area (see below). Our δ^2H values of $-184 \pm 4.9‰$ are conversely more depleted than the national average for oil and gas of $-166 \pm 6‰$ (Sherwood et al., 2017).

Our $\delta^{13}C$ values for cow breath of $-66.8 \pm 0.83‰$ are within the range of values reported for cows fed on a C_3 diet (Sherwood et al., 2017) and in close agreement with the value of $-66‰$ reported by Zazzeri et al. (2017) and the range of -71 to $-67‰$ reported by Lowry et al. (2020). Values for δ^2H from enteric fermentation have rarely been reported and range from 295‰ (Levin et al., 1993) to 358‰ (Bilek et al., 2001), encompassing our results. We are only aware of one other study, Levin et al. (1993), that has reported direct CH_4 isotope measurements from animal waste. Compared to our data, that study reported similar values for liquid manure but more enriched $\delta^{13}C$ values for manure piles. Given that over 10% of total livestock emissions are estimated to originate from manure management globally (Janssens-Maenhout et al., 2017), and around 16% in the UK according the National Atmospheric Emissions Inventory (NAEI, 2018), more data on the effect of animal waste management practices on emission signatures is needed.

The mean isotope values of $-62.4 \pm 0.87‰$ $\delta^{13}C$ and $-298 \pm 2.9‰$ δ^2H for landfill gas in this study are in good agreement with values from European landfills ($-59.0 \pm 2.2‰$ and $-304 \pm 10‰$) made by Bergamaschi et al. (1998), and with the $\delta^{13}C$ values observed during mobile surveys (Table 1). More enriched emissions ($-55 \pm 1‰$ $\delta^{13}C$) from closed landfills in the region were reported by Lowry et al. (2020). This difference may be in part explained by the fact that our samples were collected from the gas extraction system and are therefore representative of direct leaks to the atmosphere without potential oxidation in the cover soil.

There is considerable overlap in $\delta^{13}C$ values for landfills and agricultural emission sources, particularly cow breath and solid manure. However, our δ^2H values show a clear separation between landfill gas and cow breath, the main source of agricultural emissions.

4.2. Mobile CH_4 source identification

The aim of the mobile measurements was to verify the existence of potential CH_4 emission sources, as well as to identify potential gas leaks, in comparison to background levels of CH_4 throughout the study area. Elevated concentrations of CH_4 were found throughout the region (Figs. 2–4). As found in previous studies (e.g. Brandt et al., 2016; Fischer et al., 2017), emissions, as indicated by peak area, were highly right-skewed, indicating that a small fraction of sources are responsible for the majority of detected emissions (Fig. S 1). In multiple locations the isotopic signature and likely origin of notable emissions could be determined.

We detected CH_4 plumes from two out of the four managed landfills examined. On average, the $\delta^{13}C$ source signature of CH_4 plumes measured downwind of landfills was enriched by around 3‰ relative to samples collected directly from the landfill gas extraction systems (Table 1, Table S 1), though with variation between landfills. Part of the fugitive CH_4 emissions may have undergone microbial oxidation and fractionation in the cover soil, while part of the emissions may also have originated as direct emissions to the atmosphere via cracks or leakages; or from the uncovered active site of the landfill at Jameson Road where new waste was being deposited (Bergamaschi et al., 1998). Chamber measurements from capped landfill sections found no emissions from the cover soil at the sampled locations and emissions were not detected at all landfills, despite having surveyed one of them, Salt Ayre near

Lancaster, on three separate occasions. In total, these findings suggest that the combination of landfill cover and gas extraction systems employed at these sites is largely effective at limiting emissions through the cover soil, while fugitive emissions may still occur from the active site of a landfill or from, potentially preventable, leaks in the landfill cover and/or gas extraction system. Routine mobile measurements thus potentially provide a means for identifying and reducing fugitive emissions from landfills.

Four point-sources of CH_4 emissions could be identified as likely distribution pipeline gas leaks based on their thermogenic $\delta^{13}C$ signature. One source, in Lancaster city centre, was confirmed through personal communication by an on-site engineer as a gas leak known to the utility operator. The $\delta^{13}C$ values, including uncertainty estimates, of these gas leaks were within the range of values collected from a laboratory gas outlet, but notably more enriched on average (Table 1, Table S 1). It is important to note that the true number of gas pipeline leaks is possibly considerably higher as most leaks will be too small to accurately determine their isotopic value. Ground surveys using handheld gas analysers could be used to determine the source of smaller peaks identified in mobile surveys (Weller et al., 2018). Pipeline gas leaks are both a source of preventable CH_4 emissions and a potential safety hazard. While iron pipelines in the UK are gradually being replaced with less leak prone materials since 1977 (HSE, 2005) and the leaks observed in our study where not as severe as those found in mobile surveys in e.g. some US cities (Jackson et al., 2014; Phillips et al., 2013; Weller et al., 2018), identifying them so they can be monitored and repaired is still an important concern. The CH_4 detected downwind of the Barrow Gas Terminal was more enriched in ^{13}C at $-23.7 \pm 1.93‰$ than other sources. This value is possibly indicative of the isotopic signature of natural gas from the Morecambe Bay gas field, though no published isotopic values where available for comparison.

Overall, there was reasonable agreement between the mobile measurements and samples collected directly from emission sources, given the precision of $\pm 6‰$ of the mobile measurements in this study. Moreover, the combination of isotopic and wind measurements allows for source attribution in instances where concentration measurements alone might be ambiguous, such as close to landfill sites. Nonetheless, the origin of emissions can be ambiguous as isotope values for smaller or more diffuse sources, like agricultural emissions, could often not be determined with sufficient accuracy. Such limitations may be addressed with mobile sampling methods that either involve collection of discrete samples (Zazzeri et al., 2015) or systems to remeasure plumes at slower instrument speed and higher precision (Rella et al., 2015).

4.3. Land use

Investigating emissions in a region that alternates mainly between agricultural and urban land use, we expected to find overall $\delta^{13}C$ values dominated either by relatively ^{13}C depleted emissions from livestock and animal waste or relatively enriched urban gas distribution and traffic emissions (Nakagawa et al., 2005). While background concentrations were similar for both land use categories, in urban areas, $\delta^{13}C$ signatures were indeed enriched by around 1‰ compared to agricultural areas.

The overall source signature of emissions, i.e. elevated concentrations, detected during the mobile measurements, is dominated by ^{13}C-enriched thermogenic sources due to the presence of gas distribution pipeline leaks (Fig. 5). The same pattern is apparent when analysing urban and agricultural areas separately as gas leaks are present in both land use types (Fig. S 3). While this indicates that fugitive emissions from oil and gas distribution networks are an important source of CH_4 in the region, these results must be interpreted carefully as mobile, vehicle-based, measurements may not capture all sources equally in heterogeneous environments. Emissions from infrastructure, such as gas pipelines which follow the road network, can be measured close to the source, with little dispersion. Sources that are often at a distance from

public roads and/or diffuse, such as pastures, barns, slurry pits, or wetlands, will be more dispersed. Depending on sampling regime and sources present in the environment, mobile measurements may disproportionately capture road-accessible sources of CH_4 emissions, influencing total landscape level estimates.

4.4. Conclusion

Characterising CH_4 emissions in a heterogeneous environment poses challenges that typically require multiple approaches. Establishing an understanding of existing emission sources is important for future work aiming to assess the impact of potential additional sources such as shale gas production. Regional isotope data is rarely available, particularly for ^2H, while our data show that often co-located agricultural and landfill emissions differ in their δ^2H values and may therefore be distinguishable. Overall, our data demonstrate the value of utilising ^2H signatures in addition to ^{13}C for the attribution of emission sources.

Our mobile surveys indicate gas pipeline leaks and landfills as both significant and at least partially preventable sources. While land use appears to affect emission signatures, the presence of gas leaks and landfills in both urban and agricultural areas and the close proximity of different land use types confounds these differences. Overall, the combination of mobile and stationary measurements indicates that both microbial emissions, mainly from landfills and agriculture, and thermogenic CH_4 from fugitive emissions in natural gas infrastructure, contribute to total emissions in the region. Such pre-existing thermogenic emissions, which can occur randomly throughout the gas distribution network, are detectable using mobile measurements and need to be taken into account when assessing the impacts of any future gas extraction operations. Given the complexity of the CH_4 isoscape, source mapping and isotopic characterisation are key for improved understanding of spatial and temporal variation in emissions.

CRediT authorship contribution statement

Mounir Takriti: Conceptualization, Software, Methodology, Validation, Formal analysis, Data collection, Writing. **Susan E. Ward:** Conceptualization, Supervision, Project administration, Funding acquisition. **Peter M. Wynn:** Conceptualization, Supervision, Project administration. **Niall P. McNamara:** Conceptualization, Project administration, Funding acquisition, Resources, All authors provided critical feedback, discussed the results, and contributed to the final manuscript.

Declaration of competing interest

The authors declare that they have no known competing financial interests or personal relationships that could have appeared to influence the work reported in this paper.

Data availability

Datasets related to this article can be found at https://doi.org/10.5281/zenodo.4071989, an open-access data repository hosted at Zenodo (Takriti et al., 2020).

Acknowledgements

Appendix A. Supplementary data

Supplementary data to this article can be found online at https://doi.org/10.1016/j.atmosenv.2023.119774.

References

Albertson, J.D., Harvey, T., Foderaro, G., Zhu, P., Zhou, X., Ferrari, S., Amin, M.S., Modrak, M., Brantley, H., Thoma, E.D., 2016. A mobile sensing approach for regional surveillance of fugitive methane emissions in oil and gas production. Environ. Sci. Technol. 50, 2487–2497. https://doi.org/10.1021/acs.est.5b05059.

Allen, D., 2016. Attributing atmospheric methane to anthropogenic emission sources. Acc. Chem. Res. 49, 1344–1350. https://doi.org/10.1021/acs.accounts.6b00081.

Allen, D.T., 2014. Methane emissions from natural gas production and use: reconciling bottom-up and top-down measurements. Curr. Opin. Chem. Eng. 5, 78–83. https://doi.org/10.1016/j.coche.2014.05.004.

Balcombe, P., Anderson, K., Speirs, J., Brandon, N., Hawkes, A., 2017. The natural gas supply chain: the importance of methane and carbon dioxide emissions. ACS Sustain. Chem. Eng. 5, 3–20. https://doi.org/10.1021/acssuschemeng.6b00144.

Bergamaschi, P., Lubina, C., Königstedt, R., Fischer, H., Veltkamp, A.C., Zwaagstra, O., 1998. Stable isotopic signatures (δ 13 C, δD) of methane from European landfill sites. J. Geophys. Res. Atmos. 103, 8251–8265. https://doi.org/10.1029/98JD00105.

Bilek, R.S., Tyler, S.C., Kurihara, M., Yagi, K., 2001. Investigation of cattle methane production and emission over a 24-hour period using measurements of δ 13 C and δ D of emitted CH 4 and rumen water. J. Geophys. Res. Atmos. 106, 15405–15413. https://doi.org/10.1029/2001JD900177.

Brandt, A.R., Heath, G.A., Cooley, D., 2016. Methane leaks from natural gas systems follow extreme distributions. Environ. Sci. Technol. 50, 12512–12520. https://doi.org/10.1021/acs.est.6b04303.

Brantley, H.L., Thoma, E.D., Squier, W.C., Guven, B.B., Lyon, D., 2014. Assessment of methane emissions from oil and gas production pads using mobile measurements. Environ. Sci. Technol. 48, 14508–14515. https://doi.org/10.1021/es503070q.

Case, S.D.C., McNamara, N.P., Reay, D.S., Whitaker, J., 2014. Can biochar reduce soil greenhouse gas emissions from a Miscanthus bioenergy crop? GCB Bioenergy 6, 76–89. https://doi.org/10.1111/gcbb.12052.

Chang, J., Peng, S., Ciais, P., Saunois, M., Dangal, S.R.S., Herrero, M., Havlík, P., Tian, H., Bousquet, P., 2019. Revisiting enteric methane emissions from domestic ruminants and their δ13CCH4 source signature. Nat. Commun. 10, 1–14. https://doi.org/10.1038/s41467-019-11066-3.

Chanton, J.P., Powelson, D.K., Abichou, T., Fields, D., Green, R., 2008. Effect of temperature and oxidation rate on carbon-isotope fractionation during methane oxidation by landfill cover materials. Environ. Sci. Technol. 42, 7818–7823. https://doi.org/10.1021/es801221y.

Environment Agency, 2018. Historic landfill sites [WWW Document]. URL. https://data.gov.uk/dataset/17edf94f-6de3-4034-b66b-004ebd0dd010/historic-landfill-sites. (Accessed 2 November 2019).

Etminan, M., Myhre, G., Highwood, E.J., Shine, K.P., 2016. Radiative forcing of carbon dioxide, methane, and nitrous oxide: a significant revision of the methane radiative forcing. Geophys. Res. Lett. 43 (12) https://doi.org/10.1002/2016GL071930, 614-12,623.

Evans, C., Morrison, R., Burden, A., Williamson, J., Baird, A., Brown, E., Callaghan, N., Chapman, P., Cumming, A., Dean, H., Dixon, G., Dooling, G., Evans, J., Gauci, V., Grayson, R., Haddaway, N., He, Y., Heppel, K., Holden, J., Hughes, S., Kaduk, J., Jones, D., Matthews, R., Menichino, N., Misselbrook, T., Page, S., Pan, G., Peakock, M., Rayment, M., Ridley, L., Robinson, I., Rylett, D., Scowen, M., Stanley, K., Worrall, F., 2017. Final Report on Project SP1210: Lowland Peatland Systems in England and Wales – Evaluating Greenhouse Gas Fluxes and Carbon Balances.

Feinberg, A.I., Coulon, A., Stenke, A., Schwietzke, S., Peter, T., 2018. Isotopic source signatures: impact of regional variability on the δ13 CH4 trend and sp. Atmos. Environ. 174, 99–111. https://doi.org/10.1016/j.atmosenv.2017.11.037.

Fischer, J.C. von, Cooley, D., Chamberlain, S., Gaylord, A., Griebenow, C.J., Hamburg, S.P., Salo, J., Schumacher, R., Theobald, D., Ham, J., 2017. Rapid, vehicle-based identification of location and magnitude of urban natural gas pipeline leaks. Environ. Sci. Technol. 51, 4091–4099. https://doi.org/10.1021/acs.est.6b06095.

Ganesan, A.L., Schwietzke, S., Poulter, B., Arnold, T., Lan, X., Rigby, M., Vogel, F.R., van der Werf, G.R., Janssens-Maenhout, G., Boesch, H., Pandey, S., Manning, A.J., Jackson, R.B., Nisbet, E.G., Manning, M.R., 2019. Advancing scientific understanding of the global methane budget in support of the paris agreement. Global Biogeochem. Cycles 33, 1475–1512. https://doi.org/10.1029/2018GB006065.

Ganesan, A.L., Stell, A.C., Gedney, N., Comyn-Platt, E., Hayman, G., Rigby, M., Poulter, B., Hornibrook, E.R.C., 2018. Spatially resolved isotopic source signatures of wetland methane emissions. Geophys. Res. Lett. 45, 3737–3745. https://doi.org/10.1002/2018GL077536.

Hijmans, R.J., 2017. Geosphere: Spherical Trigonometry.

Hmiel, B., Petrenko, V.V., Dyonisius, M.N., Buizert, C., Smith, A.M., Place, P.F., Harth, C., Beaudette, R., Hua, Q., Yang, B., Vimont, I., Michel, S.E., Severinghaus, J.P., Etheridge, D., Bromley, T., Schmitt, J., Faïn, X., Weiss, R.F., Dlugokencky, E., 2020. Preindustrial 14CH4 indicates greater anthropogenic fossil CH4 emissions. Nature 578, 409–412. https://doi.org/10.1038/s41586-020-1991-8.

Hornibrook, E.R.C., Bowes, H.L., 2007. Trophic status impacts both the magnitude and stable carbon isotope composition of methane flux from peatlands. Geophys. Res. Lett. 34, 2–6. https://doi.org/10.1029/2007GL031231.

HSE, 2005. Enforcement Policy for the Replacement of Iron Gas Mains 2006 - 2013.

Jackson, R.B., Down, A., Phillips, N.G., Ackley, R.C., Cook, C.W., Plata, D.L., Zhao, K., Philips, N.G., Ackley, R.C., Cook, C.W., Plata, D.L., Zhao, K., 2014. Natural gas pipeline leaks across Washington, DC. Environ. Sci. Technol. 48 https://doi.org/10.1021/es404474x, 2051–8.

Janssens-Maenhout, G., Crippa, M., Guizzardi, D., Muntean, M., Schaaf, E., Dentener, F., Bergamaschi, P., Pagliari, V., Olivier, J.G.J., Peters, J.A.H.W., van Aardenne, J.A., Monni, S., Doering, U., Petrescu, A.M.R., 2017. EDGAR v4.3.2 global atlas of the three major greenhouse gas emissions for the period 1970 - 2012. Earth Syst. Sci. Data Discuss. 1–55. https://doi.org/10.5194/essd-2017-79.

Kirschke, S., Bousquet, P., Ciais, P., Saunois, M., Canadell, J.G., Dlugokencky, E.J., Bergamaschi, P., Bergmann, D., Blake, D.R., Bruhwiler, L., Cameron-Smith, P., Castaldi, S., Chevallier, F., Feng, L., Fraser, A., Heimann, M., Hodson, E.L., Houweling, S., Josse, B., Fraser, P.J., Krummel, P.B., Lamarque, J.-F., Langenfelds, R. L., Le Quéré, C., Naik, V., O'Doherty, S., Palmer, P.I., Pison, I., Plummer, D., Poulter, B., Prinn, R.G., Rigby, M., Ringeval, B., Santini, M., Schmidt, M., Shindell, D. T., Simpson, I.J., Spahni, R., Steele, L.P., Strode, S.A., Sudo, K., Szopa, S., van der Werf, G.R., Voulgarakis, A., van Weele, M., Weiss, R.F., Williams, J.E., Zeng, G., 2013. Three decades of global methane sources and sinks. Nat. Geosci. 6, 813–823. https://doi.org/10.1038/ngeo1955.

Legendre, P., 2018. lmodel2: Model II Regression.

Levin, I., Bergamaschi, P., Dörr, H., Trapp, D., 1993. Stable isotopic signature of methane from major sources in Germany. Chemosphere 26, 161–177. https://doi.org/10.1016/0045-6535(93)90419-6.

Liu, Q., Wu, X., Wang, X., Jin, Z., Zhu, D., Meng, Q., Huang, S., Liu, J., Fu, Q., 2019. Carbon and hydrogen isotopes of methane, ethane, and propane: a review of genetic identification of natural gas. Earth Sci. Rev. 190, 247–272. https://doi.org/10.1016/j.earscirev.2018.11.017.

Lopez, M., Sherwood, O.A., Dlugokencky, E.J., Kessler, R., Giroux, L., Worthy, D.E.J., 2017. Isotopic signatures of anthropogenic CH4 sources in Alberta, Canada. Atmos. Environ. Times 164, 280–288. https://doi.org/10.1016/j.atmosenv.2017.06.021.

Lowry, D., Fisher, R.E., France, J.L., Coleman, M., Lanoisellé, M., Zazzeri, G., Nisbet, E. G., Shaw, J.T., Allen, G., Pitt, J., Ward, R.S., 2020. Environmental baseline monitoring for shale gas development in the UK: identification and geochemical characterisation of local source emissions of methane to atmosphere. Sci. Total Environ. 708, 134600 https://doi.org/10.1016/j.scitotenv.2019.134600.

McEwing, K.R., Fisher, J.P., Zona, D., 2015. Environmental and vegetation controls on the spatial variability of CH4 emission from wet-sedge and tussock tundra ecosystems in the Arctic. Plant Soil 388, 37–52. https://doi.org/10.1007/s11104-014-2377-1.

Miller, J.B., Tans, P.P., 2003. Calculating isotopic fractionation from atmospheric measurements at various scales. Tellus Ser. B Chem. Phys. Meteorol. 55, 207–214. https://doi.org/10.1034/j.1600-0889.2003.00020.x.

NAEI, 2018. National atmospheric emissions inventory [WWW Document]. URL. http://naei.beis.gov.uk/. (Accessed 9 May 2018).

Nakagawa, F., Tsunogai, U., Komatsu, D.D., Yamada, K., Yoshida, N., Moriizumi, J., Nagamine, K., Iida, T., Ikebe, Y., 2005. Automobile exhaust as a source of 13C- and D-enriched atmospheric methane in urban areas. Org. Geochem. 36, 727–738. https://doi.org/10.1016/j.orggeochem.2005.01.003.

Phillips, N.G., Ackley, R., Crosson, E.R., Down, A., Hutyra, L.R., Brondfield, M., Karr, J. D., Zhao, K., Jackson, R.B., 2013. Mapping urban pipeline leaks: methane leaks across Boston. Environ. Pollut. 173, 1–4. https://doi.org/10.1016/j.envpol.2012.11.003.

Rella, C.W., Hoffnagle, J., He, Y., Tajima, S., 2015. Local- and regional-scale measurements of CH4, δ13CH4, and C2H6 in the Uintah Basin using a mobile stable isotope analyzer. Atmos. Meas. Tech. 8, 4539–4559. https://doi.org/10.5194/amt-8-4539-2015.

Rowland, C.S., Morton, R.D., Carrasco, L., McShane, G., O'Neil, A.W., Wood, C.M., 2017. Land Cover Map 2015 (Vector, GB). NERC Environmental Information Data Centre. https://doi.org/10.5285/6c6c9203-7333-4d96-88ab-78925e7a4e73.

Saunois, M., Bousquet, P., Poulter, B., Peregon, A., Ciais, P., Canadell, J.G., Dlugokencky, E.J., Etiope, G., Bastviken, D., Houweling, S., Janssens-Maenhout, G., Tubiello, F.N., Castaldi, S., Jackson, R.B., Alexe, M., Arora, V.K., Beerling, D.J., Bergamaschi, P., Blake, D.R., Brailsford, G., Brovkin, V., Bruhwiler, L., Crevoisier, C., Crill, P., Covey, K., Curry, C., Frankenberg, C., Gedney, N., Höglund-Isaksson, L., Ishizawa, M., Ito, A., Joos, F., Kim, H.S., Kleinen, T., Krummel, P., Lamarque, J.F., Langenfelds, R., Locatelli, R., Machida, T., Maksyutov, S., McDonald, K.C., Marshall, J., Melton, J.R., Morino, I., Naik, V., O'Doherty, S., Parmentier, F.J.W., Patra, P.K., Peng, C., Peng, S., Peters, G.P., Pison, I., Prigent, C., Prinn, R., Ramonet, M., Riley, W.J., Saito, M., Santini, M., Schroeder, R., Simpson, I.J., Spahni, R., Steele, P., Takizawa, A., Thornton, B.F., Tian, H., Tohjima, Y., Viovy, N.,

Voulgarakis, A., Van Weele, M., Van Der Werf, G.R., Weiss, R., Wiedinmyer, C., Wilton, D.J., Wiltshire, A., Worthy, D., Wunch, D., Xu, X., Yoshida, Y., Zhang, B., Zhang, Z., Zhu, Q., 2016. The global methane budget 2000-2012. Earth Syst. Sci. Data 8, 697–751. https://doi.org/10.5194/essd-8-697-2016.

Saunois, M., Stavert, A.R., Poulter, B., Bousquet, P., Canadell, J.G., Jackson, R.B., Raymond, P.A., Dlugokencky, E.J., Houweling, S., Patra, P.K., Ciais, P., Arora, V.K., Bastviken, D., Bergamaschi, P., Blake, D.R., Brailsford, G., Bruhwiler, L., Carlson, K. M., Carrol, M., Castaldi, S., Chandra, N., Crevoisier, C., Crill, P.M., Covey, K., Curry, C.L., Etiope, G., Frankenberg, C., Gedney, N., Hegglin, M.I., Höglund-Isaksson, L., Hugelius, G., Ishizawa, M., Ito, A., Janssens-Maenhout, G., Jensen, K.M., Joos, F., Kleinen, T., Krummel, P.B., Langenfelds, R.L., Laruelle, G.G., Liu, L., Machida, T., Maksyutov, S., McDonald, K.C., McNorton, J., Miller, P.A., Melton, J.R., Morino, I., Müller, J., Murguia-Flores, F., Naik, V., Niwa, Y., Noce, S., O'Doherty, S., Parker, R.J., Peng, C., Peng, S., Peters, G.P., Prigent, C., Prinn, R., Ramonet, M., Regnier, P., Riley, W.J., Rosentreter, J.A., Segers, A., Simpson, I.J., Shi, H., Smith, S. J., Steele, L.P., Thornton, B.F., Tian, H., Tohjima, Y., Tubiello, F.N., Tsuruta, A., Viovy, N., Voulgarakis, A., Weber, T.S., van Weele, M., van der Werf, G.R., Weiss, R. F., Worthy, D., Wunch, D., Yin, Y., Yoshida, Y., Zhang, W., Zhang, Z., Zhao, Y., Zheng, B., Zhu, Qing, Zhu, Qiuan, Zhuang, Q., 2020. The global methane budget 2000–2017. Earth Syst. Sci. Data 12, 1561–1623. https://doi.org/10.5194/essd-12-1561-2020.

Schwietzke, S., Sherwood, O.A., Bruhwiler, L.M.P., Miller, J.B., Etiope, G., Dlugokencky, E.J., Michel, S.E., Arling, V.A., Vaughn, B.H., White, J.W.C., Tans, P. P., 2016. Upward revision of global fossil fuel methane emissions based on isotope database. Nature 538, 88–91. https://doi.org/10.1038/nature19797.

Sherwood, O.A., Schwietzke, S., Arling, V.A., Etiope, G., 2017. Global inventory of gas geochemistry data from fossil fuel, microbial and burning sources, version 2017. Earth Syst. Sci. Data 9, 639–656. https://doi.org/10.5194/essd-9-639-2017.

Shindell, D., Kuylenstierna, J.C.I., Vignati, E., van Dingenen, R., Amann, M., Klimont, Z., Anenberg, S.C., Muller, N., Janssens-Maenhout, G., Raes, F., Schwartz, J., Faluvegi, G., Pozzoli, L., Kupiainen, K., Hoglund-Isaksson, L., Emberson, L., Streets, D., Ramanathan, V., Hicks, K., Oanh, N.T.K., Milly, G., Williams, M., Demkine, V., Fowler, D., 2012. Simultaneously mitigating near-term climate change and improving human health and food security. Science 335, 183–189. https://doi.org/10.1126/science.1210026, 80–.

Takriti, M., Wynn, P.M., Elias, D.M.O., Ward, S.E., Oakley, S., McNamara, N.P., 2020. North West England mobile methane concentration and isotope measurements (1.0). Zenodo. https://doi.org/10.5281/zenodo.4071990.

Takriti, M., Wynn, P.M., Elias, D.M.O., Ward, S.E., Oakley, S., McNamara, N.P., 2021. Mobile methane measurements: effects of instrument specifications on data interpretation, reproducibility, and isotopic precision. Atmos. Environ. 246, 118067 https://doi.org/10.1016/j.atmosenv.2020.118067.

Turner, A.J., Frankenberg, C., Wennberg, P.O., Jacob, D.J., 2017. Ambiguity in the causes for decadal trends in atmospheric methane and hydroxyl. Proc. Natl. Acad. Sci. USA 114, 5367–5372. https://doi.org/10.1073/pnas.1616020114.

Vavrek, M.J., 2011. fossil: palaeoecological and palaeogeographical analysis tools. Palaeontol. Electron. 14, 1T.

Vermeesch, P., 2018. IsoplotR: a free and open toolbox for geochronology. Geosci. Front. https://doi.org/10.1016/j.gsf.2018.04.001.

Wehr, R., Saleska, S.R., 2017. The long-solved problem of the best-fit straight line: application to isotopic mixing lines. Biogeosciences 14, 17–29. https://doi.org/10.5194/bg-14-17-2017.

Weller, Z.D., Roscioli, J.R., Daube, W.C., Lamb, B.K., Ferrara, T.W., Brewer, P.E., Von Fischer, J.C., 2018. Vehicle-based methane surveys for finding natural gas leaks and estimating their size: validation and uncertainty. Environ. Sci. Technol. 52, 11922–11930. https://doi.org/10.1021/acs.est.8b03135.

Whiticar, M.J., 1999. Carbon and hydrogen isotope systematics of bacterial formation and oxidation of methane. Chem. Geol. 161, 291–314. https://doi.org/10.1016/S0009-2541(99)00092-3.

Xueref-Remy, I., Zazzeri, G., Bréon, F.M., Vogel, F., Ciais, P., Lowry, D., Nisbet, E.G., 2020. Anthropogenic methane plume detection from point sources in the Paris megacity area and characterization of their δ13C signature. Atmos. Environ. 222, 117055 https://doi.org/10.1016/j.atmosenv.2019.117055.

Xueref-Remy, I., Zazzeri, G., Bréon, F.M., Vogel, F., Ciais, P., Lowry, D., Nisbet, E.G., 2019. Anthropogenic methane plume detection from point sources in the Paris megacity area and characterization of their δ13C signature. Atmos. Environ., 117055 https://doi.org/10.1016/j.atmosenv.2019.117055.

Yarnes, C., 2013. δ13C and δ2H measurement of methane from ecological and geological sources by gas chromatography/combustion/pyrolysis isotope-ratio mass spectrometry. Rapid Commun. Mass Spectrom. 27, 1036–1044. https://doi.org/10.1002/rcm.6549.

York, D., 1969. Least squares fitting of a straight line with correlated errors. Earth Planet Sci. Lett. 5, 320–324. https://doi.org/10.1016/S0012-821X(68)80059-7.

Zazzeri, G., Lowry, D., Fisher, R.E., France, J.L., Lanoisellé, M., Grimmond, C.S.B., Nisbet, E.G., 2017. Evaluating methane inventories by isotopic analysis in the London region. Sci. Rep. 7, 4854. https://doi.org/10.1038/s41598-017-04802-6.

Zazzeri, G., Lowry, D., Fisher, R.E., France, J.L., Lanoisellé, M., Nisbet, E.G., 2015. Plume mapping and isotopic characterisation of anthropogenic methane sources. Atmos. Environ. 110, 151–162. https://doi.org/10.1016/j.atmosenv.2015.03.029.